Springer

KSME

Journal of Mechanical Science and Technology 31 (9) (2017) 4221~4226
www.springerlink.com/content/1738-494x(Print)/1976-3824(Online)
DOI 10.1007/s12206-017-0820-y

Aerodynamic performance optimization for the rotor design of a hovering agricultural unmanned helicopter †

B. A. Haider[1], C. H. Sohn[1,*], Y. S. Won[2] and Y. M. Koo[2,*]

[1]*School of Mechanical Engineering, Kyungpook National University, Daegu 41566, Korea*
[2]*School of Agricultural Civil and Bio-Industrial Engineering, Kyungpook National University, Daegu 41566, Korea*

(Manuscript Received October 18, 2016; Revised April 20, 2017; Accepted May 15, 2017)

Abstract

The importance of using Agriculture unmanned helicopters (AUHs), especially for spraying pesticides and fertilizers on any terrain type to ensure crop yields, has been recently acknowledged. Apart from flying these helicopters at a super-low altitude and low speed, using an efficient and optimum rotor blade ensures a uniform and deep penetration of pesticide and fertilizers over a specified area. Accordingly, this work attempts to optimize the rotor blade of an AUH by using coupling statistics and several numerical techniques, including design of experiments, response surface method, and computational fluid dynamics. The experiments are designed using the central composite design method and by selecting the geometric variables that affect the aerodynamic performance of the rotor blade, including the root chord, tip chord, and angle of attack. The angle at the root and tip is optimized in order for the resulting twist to produce a uniform blade loading, achieve maximum lift, and minimize the required hover power. The required aerodynamic forces and limited availability of engine power are identified as constraints. The blade is optimized only when the helicopter is hovering at a persistent rotational speed, and the hover efficiency of the rotor blade with an optimal twist distribution is significantly higher than the baseline.

Keywords: Agricultural unmanned helicopter; Design of experiments; Hover performance; Multi-objective optimization; Response surface method; Rotor blade

1. Introduction

The application of airborne systems in agriculture, especially unmanned helicopters, has flourished in recent years [1, 2]. Agriculture unmanned helicopters (AUHs) greatly outperform fixed-wing aircrafts in terms of hovering, vertical take-off and landing, low runway requirements, and ability to fly at low speed and altitude, thereby making these helicopters suitable tools for agricultural production. These helicopters have also been identified as viable, economical, and potential tools for remote sensing and high-resolution photography that can help improve the existing agricultural practices and make agriculture-related decisions [3]. Accordingly, farmers have begun to use AUHs in applying precise amounts of seed, water, herbicide, and pesticide to ensure favorable crop yields.

In addition to their remote sensing applications, AUHs have also been used for spraying chemicals [4, 5], which is considered a harmful and labor-intensive task in agriculture. In this way, AUHs can significantly address those concerns related to farming labor, health, and environment. AUHs also ensure a timely and accurate application of these chemicals, thereby minimizing incidents of drift loss and evaporation. The downwash from the helicopter rotor also ensures the uniform and deep penetration of pesticides.

AUHs are generally smaller than full-scale commercial manned helicopters yet have the same main parts, among which the main rotor produces the aerodynamic forces. Thus, the rotor blade must be carefully designed to ensure the optimal performance of AUHs in all flight conditions, especially when hovering.

However, rotorcraft design and optimization are challenging tasks. Rotor blades are also surrounded by an unsteady flow resulting from the different flow conditions that they encounter per blade revolution. Different flight regimes also impose various design requirements that make the optimization problem multi-objective and multidisciplinary. All these aspects must be considered concurrently such as in Refs. [6, 7].

As an efficient and robust tool, the Response surface methodology (RSM) has been extensively applied in the optimization process [8-11]. RSM comprises a group of mathematical and statistical techniques that are useful for design and optimization processes, experiments, regression analyses, and analyses of variance [12].

This paper aims to describe an optimization process where RMS is applied to the rotor blade of an existing AUH to im-

*Corresponding author. Tel.: +82 53 950 5570, 5788, Fax.: +82 53 950 6550
E-mail address: chsohn@knu.ac.kr, ymkoo@knu.ac.kr
† Recommended by Associate Editor Kyu Hong Kim

Fig. 1. AUH employed in this study (AgroHeli-4G).

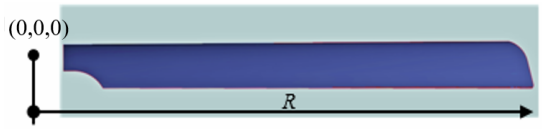

Fig. 2. Rotor blade geometry (*R* is the blade radius).

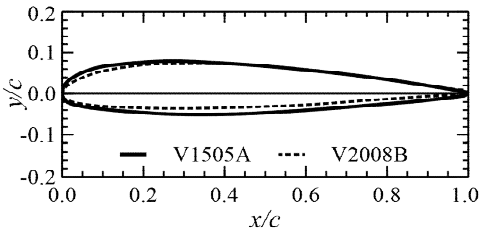

Fig. 3. Rotor blade airfoil sections.

prove its aerodynamic performance. To obtain an optimum blade, the twist angle is optimized by varying the pitch angles at the root and tip, changing the tip chord length, and keeping the root chord length unchanged. A Computational fluid dynamics (CFD) analysis is performed using a 3D Navier-Stokes solver. The hover flight condition is considered for blade optimization because the AUH spends most of its time hovering at a relatively low speed (approximately 4 m/s to 7 m/s) at an altitude of 2 m to 4 m [5, 13].

2. Computational methodology

Fig. 1 shows the AUH employed in this study, AgroHeli-4G (AH-4G), which comprises two rectangular blades with a root cut-out, a parabolic tip shape (see Fig. 2), and an angular rotating speed of 890 rpm [14, 15]. AH-4G has a 1176 N maximum lift capacity, 25 kW engine rated power, and 650 N total dead weight, while its blades have an aspect ratio of 11.185 with a linear twist of -5°. These blades are based on two airfoil sections, namely, V1505A and V2008B, which are located at the root and tip, respectively. The inboard profile (V1505A) is a relatively thick airfoil section with a blunt nose, while the outboard profile (V2008B) is a relatively thin airfoil section with a drooped leading edge. V1505A is suitable for the inboard section and is aerodynamically more stable than V2008B because of its gradual stall, while V2008B is suitable for the outboard section and shows a relatively higher dynamic efficiency than V1505A. The airfoil sections are superimposed in Fig. 3. The blade geometry is modeled parametrically by varying the design variables, namely, the angles at the root and tip and the chord length of the tip.

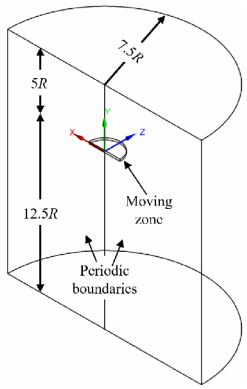

Fig. 4. Computational domain with boundary conditions.

The computational domain for the CFD analysis of the rotor blade involves a half cylinder (stationary fluid zone) and a single blade contained in a circular disk (moving fluid zone). Only one blade is considered due to rotational periodicity. Fig. 4 shows the computational domain with boundary extents and the corresponding boundary conditions. The speed of the moving fluid zone at the clockwise direction of the negative y-axis is fixed at 890 rpm. The far-field boundary condition with ambient properties is imposed on the outer boundary of the stationary fluid zone, while the no-slip boundary condition is applied to the blade surface. An interface is also defined between the moving and stationary fluid zones. An unstructured mesh is generated for the whole fluid domain and blade surfaces. Unstructured meshing provides flexibility in grid generation and is widely used in helicopter rotor blade simulations [16].

In this study, the Reynolds-averaged Navier-Stokes equations are solved in conjunction with the multiple reference frame method for an isolated rotor blade. The computations are performed using Ansys Fluent solver [17]. The isolated rotor in hovering flight exhibits a steady-state flow in the moving reference frame. The realizable k-epsilon turbulence model is employed with an enhanced wall treatment.

A grid sensitivity test is also performed to obtain a grid-independent solution. Three grids of 1.2, 2.4 and 4.8 million elements are considered. The rotor blade tested by Caradonna and Tung [18] is utilized for examining grid independence, and the same methodology is applied to the rotor blade in question. Fig. 5 compares the computed chordwise pressure distribution with the experimental data for various grid sizes. All grids agree well with one another and with the experiment results, thereby validating the applied method. A grid size of 2.4 million is used for the subsequent analysis.

3. Response surface optimization

3.1 RSM

RSM consists of mathematical and statistical techniques for

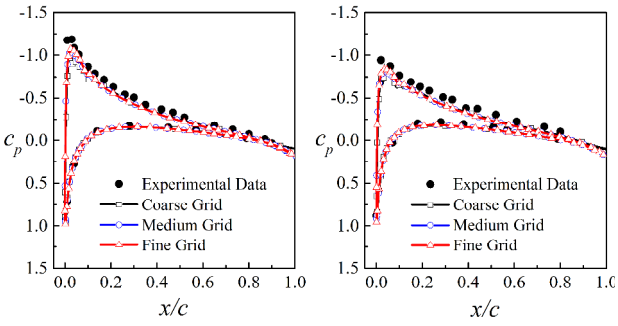

(a) $r/R = 0.68$ (b) $r/R = 0.89$

Fig. 5. Comparison of the numerically computed chordwise pressure distribution for various grids with the experimental data [18].

approximating modeling problems [12]. In the RSM framework, single or multiple response (output) variables are described in terms of several independent (input) variables in the form of a polynomial fit or a neural network. The design of experiments method is employed to build the response functions and to rapidly provide the approximated values of the response variables in the computed design space without having to provide a complete solution. The relationship among the response variables can be linearly expressed as follows:

$$y = b_0 + \sum_{i=1}^{N} b_i x_i + \varepsilon \,, \tag{1}$$

where N is the number of variables, b_0 is a constant term, b_i denotes the coefficients of the linear variables, and ε represents the residual related to the experiments which are often assumed to have a normal distribution with a zero mean. To model the second-order interactions among the variables, the empirical model is expressed in a quadratic form as follows based on RSM:

$$y = b_0 + \sum_{i=1}^{N} b_i x_i + \sum_{i=1}^{N}\sum_{j=1}^{N} b_{ij} x_i x_j + \varepsilon \,, \tag{2}$$

where b_{ij} denotes the coefficients of the interaction variables which are usually computed via least-square regression analysis. The quadratic empirical model can be expressed in matrix notation as follows:

$$y = \mathbf{X}b + \varepsilon \,. \tag{3}$$

The coefficients are obtained by minimizing the least square error as follows:

$$\hat{b} = \left(\mathbf{X}^{\mathrm{T}}\mathbf{X}\right)^{-1}\mathbf{X}^{\mathrm{T}} y \,. \tag{4}$$

The fitted regression model is eventually obtained as follows:

Table 1. Levels of design variables with the corresponding coded and physical symbols.

Design variables (coded)	Symbols (physical)	Levels		
		-1	0	1
x_1 (deg)	θ_r	5	15	25
x_2 (deg)	θ_t	-5	5	15
x_3 (m)	c_t	0.1000	0.1175	0.1350

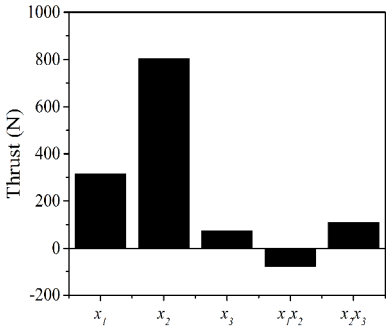

Fig. 6. Effect of the design variables and their interaction on thrust.

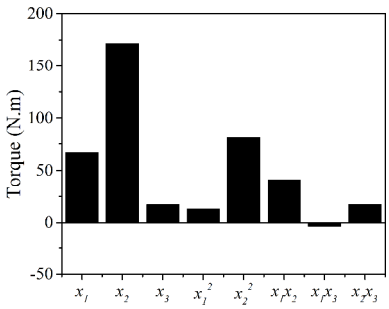

Fig. 7. Effect of the design variables and their interaction on torque.

$$\hat{y} = X\hat{b} \,. \tag{5}$$

3.2 Sensitivity analysis

The variables and their interactions are then subjected to a sensitivity analysis. The signs of the effects are not significant for the comparison, but their magnitude drives the response of the system. The effect of a variable is computed as follows:

$$\text{Effect of variable} = \frac{\text{Contrast}}{n2^{k-1}} \,, \tag{6}$$

where n is a replication of the results ($n = 1$, k-1 = 2).

The design variables considered in this study include the pitch angle at the root section, x_1, the pitch angle at the tip section, x_2, and the tip chord length, x_3. These parameters are varied within the prescribed upper and lower bounds presented in Table 1. Given that the level of pitch angles at both sections are constrained, the combination of both may produce a negative twist.

Figs. 6 and 7 show that thrust and torque are highly sensi-

tive to tip angle. Pitch angle has the second most significant effect on the response parameters, whereas tip chord shows a minimal effect on the performance variables. The interaction among the design variables reflects the significance of the torque computation, especially the product of the pitch angles at the root and tip, whereas thrust shows limited sensitivity to such interactions.

3.3 Optimization problem

This study aims to obtain an optimum rotor blade with a maximum hover efficiency. The Figure of merit (*FM*) can be obtained either by maximizing the thrust (*T*) or minimizing the torque (*Q*).

This multi-objective problem can be expressed as follows:

$$\text{Maximize: } \{T\} \text{ and Minimize: } \{Q\}$$

Subject to:

$$\left.\begin{aligned} x_{1,\text{lower}} \le x_1 \le x_{1,\text{upper}} \\ x_{2,\text{lower}} \le x_2 \le x_{2,\text{upper}} \end{aligned}\right\} \text{ such that } x_1 > x_2$$

$$x_{3,\text{lower}} \le x_3 \le x_{3,\text{upper}} .$$

3.4 Generation of response surface

Using the helicopter computational analysis, the objective functions *T* and *Q* are evaluated in the design space corresponding to a face-centered central composite design (CCF) in which $\alpha = 1$, where α is the distance of each axial point (also called star point) from the center of a central composite design. The CCF consists of one center point, $2N$ points located at the $-\alpha$ and $+\alpha$ positions on each axis of the selected input variable, and 2^{N+f} factorial points ($f = 0$) located at the -1 and +1 positions along the diagonals of the input variables. To simplify the calculations, the independent variables are coded to the usual ($-\alpha$, α) interval. Table 2 presents the results for thrust and torque with the coded values of the design variables x_1, x_2 and x_3. Fig. 8 shows the relation of each response variable for the whole design space.

By minimizing the square of the error, the resulting response surface models for thrust and torque in physical units are computed as follows:

$$\begin{aligned} T = {} & 62.7 + 17.71x_1 + 9.03x_2 + 534x_3 \\ & -0.382x_1x_2 + 314.5x_2x_3 \end{aligned} \tag{7}$$

$$\begin{aligned} Q = {} & -12.69 + 1.524x_1 - 4.392x_2 + 381.5x_3 \\ & +0.0643x_1^2 + 0.4042x_2^2 + 0.20614x_1x_2 \\ & -9.62x_1x_3 + 49.68x_2x_3 \end{aligned} \tag{8}$$

The accuracy of the response surface must be estimated because the model is based on an approximation of the computational results. Therefore, Table 3 examines the goodness of fit of thrust and torque. In this way, the variation in the blade performance parameters resulting from the changes in the design variables can be predicted accurately.

Table 2. Design of experiments table generated using CCF with the corresponding response values.

Run	x_1	x_2	x_3	*T* (N)	Q (N. m)
1	-1	-1	-1	2.633	30.596
2	1	-1	-1	402.655	60.740
3	-1	1	-1	790.953	144.401
4	1	1	-1	985.188	256.297
5	-1	-1	1	14.096	35.637
6	1	-1	1	338.832	58.605
7	-1	1	1	933.440	183.639
8	1	1	1	1204.520	288.343
9	-1	0	0	382.544	58.878
10	1	0	0	822.298	123.655
11	0	-1	0	165.376	40.030
12	0	1	0	1065.920	210.484
13	0	0	-1	584.292	81.041
14	0	0	1	614.017	89.902
15	0	0	0	603.253	85.536

Table 3. Goodness of fit in rotor blade design.

Response variables	R^2	R^2_{adj}
Thrust (N)	0.993	0.983
Torque (N. m)	1.000	1.000

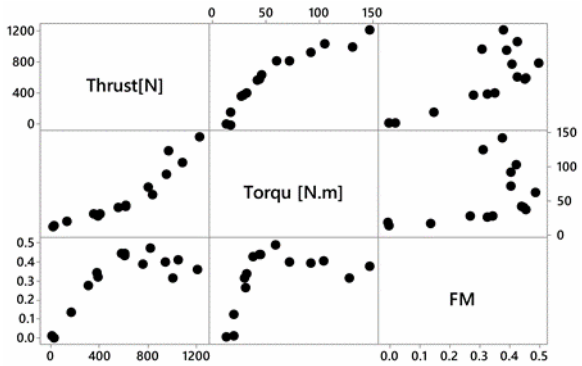

Fig. 8. Matrix plot of the response parameters.

3.5 Optimization results

Multi-objective optimization is conducted using the response surface model. An exhaustive search is conducted in the design space to maximize the thrust and minimize the torque. The combination of these two parameters eventually increases FM. Some excellent designs are obtained using the response surface approximation. The design point 1 (x_1 = 24.2°, x_2 = 11.09° and x_3 = 0.134) is the best design obtained through multi-objective optimization that increases FM by 12 %. Table 9 compares the design points with the baseline, while Figs. 9 and 10 show the thrust and torque in the re-

Table 4. Comparison of the baseline with the design points obtained through the response surface method using multi-objective optimization.

Parameters	Baseline	Design point 1	Design point 2	Design point 3
x_1 (deg)	18	24.20	19.75	19.68
x_2 (deg)	13	11.09	11.66	12.60
x_3 (m)	0.135	0.134	0.135	0.135
Twist (deg)	-5.00	-13.11	-8.09	-7.08
T (N)	1090	1128 (3.5 %) ↑	1063 (2.5 %) ↓	1103 (1.2 %)↑
Q (N.m)	199	186 (6.5 %) ↓	181 (9.1 %) ↓	192 (3.5 %) ↓
P (kW)	18.60	17.42	16.86	17.90
FM	0.4628	0.5191	0.4931	0.4890
		(12 %) ↑	(6.5 %) ↑	(5.6 %) ↑

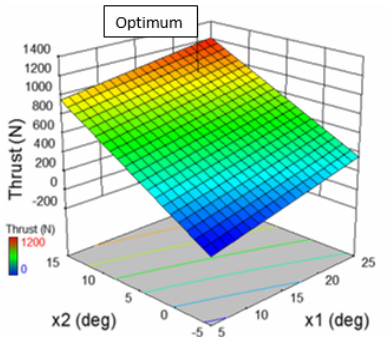

Fig. 9. Variation of thrust with respect to pitch angle at the root and tip with the tip chord held constant at the design value.

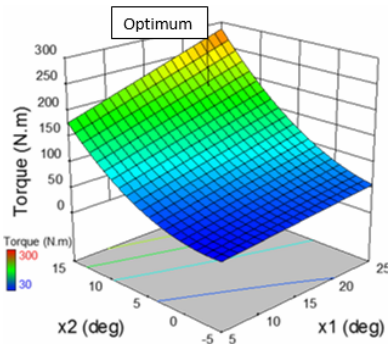

Fig. 10. Variation of torque with respect to pitch angle at the root and tip with the tip chord held constant at the design value.

sponse surfaces.

Table 4 shows that FM varies from 0.46 to 0.52 for the baseline and optimum design, respectively. However, these values are relatively lower than the FM of modern commercial full-scale helicopters (0.7 or higher). AUHs have a high induced power because they operate at a very low speed (approximately 4 m/s to 7 m/s) and maintain a hovering flight. Lee et al. [19] observed the similar problem, where the value of FM is approximately 0.60 with a large induced power factor (1.35 to 1.42) that is higher than that of a full-scale helicopter (1.15). By contrast, the induced power factor recorded in this study was 1.5.

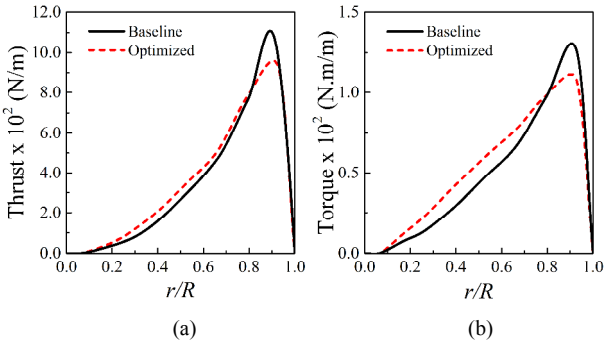

Fig. 11. Comparison of the spanwise aerodynamic loading of the baseline and optimal design: (a) Sectional thrust per unit span; (b) sectional torque per unit span.

Fig. 11 compares the spanwise variation of the thrust and torque of the baseline design to the blades that are obtained through response surface optimization. The blade loading for the optimized design is in a quadratic form because the twist is linearly distributed. However, a highly uniform torque distribution is observed in the optimized blade with an improved hover efficiency. Fig. 11 shows a reduction in tip loading and a significant improvement in the design.

4. Conclusions

A parametric study was performed to improve the hover efficiency of an AUH. The effect of the rotor blade design variables on hover efficiency was analyzed. Using the design of experiments technique, 15 experiments were designed based on three variables through the CCD approach. Reynolds-averaged Navier-Stokes equations with a multiple reference frame were solved to simulate the designs. The statistical analysis reveals that the angles at the root and pitch were highly sensitive to thrust and torque and that chord length had a minimal effect on the response variables. Some excellent designs were obtained by employing RSM. Among these designs, an optimized rotor blade with a twist of -13.11° showed a 3.5 % improvement in thrust, 6.5 % reduction in torque, and 12 % improvement in hover efficiency or *FM*. The *FM* value varied from 0.46 to 0.52 for the baseline and optimum design, but this value is relatively lower than that of modern commercial full-scale helicopters (0.7 or higher). This study only analyzed a small-scale two-bladed agricultural helicopter rotor, and the reference efficiency and performance of similar helicopters designs remain unexplored in the literature to the best of the knowledge of the authors.

Acknowledgment

This work was supported by the National Research Foundation of Korea (NRF) and funded by the Ministry of Science, ICT & Future Planning (Grant No. 2015R1A2A2A01002328).

References

[1] R. C. Amsden, The use of helicopter in agriculture, *Outlook on Agriculture,* 15 (1986) 61-64.

[2] J. Zhou, L. R. Khot, T. Peters, M. D. Whiting, Q. Zhang and D. Granatstein, Efficacy of unmanned helicopter in rainwater removal from cherry canopies, *Computers and Electronics in Agriculture*, 124 (2016) 161-167.

[3] C. Zhang and J. Kovacs, The application of small unmanned aerial systems for precision agriculture: A review, *Precision Agriculture,* 13 (2012) 693-712.

[4] Y. M. Koo, C. S. Lee, T. S. Soek, S. K. Shin, T. G. Kang, S. H. Kim and T. Y. Choi, Aerial application using a small RF controlled helicopter (I)-status and cost analysis, *Journal of Biosystems Engineering*, 31 (2006) 95-101.

[5] T. Meng, Exploration and practice for the agricultural value of unmanned helicopters, *Electronics, Information Technology and Intellectualization* (2015) 191-194.

[6] H. M. Adelman and W. R. Mantay, Integrated multidisciplinary optimization of rotorcraft: A plan for development, *Technical Report NASA-TM-101617*, NASA (1989).

[7] M. Imiela, High-fidelity optimization framework for helicopter rotors, *Journal of Aerospace Science and Technology*, 23 (2012) 2-16.

[8] K. K. Saijal and R. Ganguli, Optimization of helicopter rotor using polynomial and neural network metamodels, *Journal of Aircraft*, 48 (2011) 553-566.

[9] H. Sun and S. Lee, Response surface approach to aerodynamic optimization design of helicopter rotor blade, *International Journal for Numerical Methods in Engineering*, 64 (2005) 125-142.

[10] H. Sun, Wind turbine airfoil design using response surface method, *Journal of Mechanical Science and Technology,* 25 (2011) 1335-1340.

[11] E. Adeeb, A. Maqsood, A. Musthaq and C. H. Sohn, Parametric study and optimization of ceiling fan blades for improved aerodynamic performance, *Journal of Applied Fluid Mechanics,* 9 (2016) 2905-2916.

[12] R. H. Myers and D. C. Montgomery, *Response surface methodology: Process and product optimization using designed experiments*, Wiley, New York (1995).

[13] Y. M. Koo, T. S. Soek, S. K. Shin, C. S. Lee and T. G. Kang, Aerial application using a small RF controlled helicopter (III) - lift test and rotor system, *Journal of Biosystems Engineering*, 31 (2006) 182-187.

[14] Y. M. Koo, Development of essential mechanical elements for unmanned agricultural helicopter with payload of 20 kg, *Final Report for IUPL of SMBA*, MOCIE, Daegu, Korea (2009).

[15] Y. M. Koo, Performance comparison of two airfoil rotor designs for an agricultural unmanned helicopter, *Journal of Biosystems Engineering*, 37 (2012).

[16] B. A. Haider, C. H. Sohn, Y. S. Won and Y. M. Koo, Aerodynamically efficient rotor design for hovering agricultural unmanned helicopter, *Journal of Applied Fluid Mechanics,* 10 (2017).

[17] Ansys Fluent Release 16.2, ANSYS® Academic Research, Help System, *Fluent Theory and User's Guide*, ANSYS Inc (2016).

[18] F. Caradonna and C. Tung, Experimental and analytical studies of a model helicopter rotor in hover, *Technical Report NASA-TM-81232*, NASA (1981).

[19] B. E. Lee, Y. S. Byun, J. Kim and B. S. Kang, Experimental performance evaluation on a small-scale rotor using a rotor test stand, *The Journal of Mechanical Science and Technology*, 25 (2011) 1449-1456.

Basharat Ali Haider received his M.Sc. in Mechanical Engineering from the University of Belgrade, Serbia in 2009. He is currently a Ph.D. student at Kyungpook National University, Daegu, South Korea. His research interests include computational fluid dynamics, aerodynamic design and optimization, immersed boundary method, lattice Boltzmann method, and fluid-structure interaction.

Chang Hyun Sohn received his M.Sc. and Ph.D. in Mechanical Engineering from KAIST in 1985 and 1991, respectively. He worked in ADD for three years and as a Visiting Assistant Professor in the University of Cambridge in 1996. Dr. Sohn is currently a Professor at the Department of Mechanical Engineering at Kyungpook National University, Daegu, South Korea. His research interests include computational fluid dynamics, particle image velocimetry, flow induced vibration, and thermal hydraulics.

Yong Sik Won received his B.Sc. in Bio-industrial Machinery Engineering from Kyungpook National University, Daegu, South Korea. He is currently a master student in Bio-Industrial Machinery Engineering at Kyungpook National University, Daegu, South Korea. His research interests include computational fluid dynamics and helicopter rotor blade design.

Young Mo Koo received his M.Sc. in Bio & Agricultural Engineering from Rutgers, The State University of New Jersey, USA. He then received his Ph.D. in Agricultural Engineering from Kansas State University, USA. Dr. Koo is currently a Professor at the Department of Bio-Industrial Machinery Engineering at Kyungpook National University, Daegu, South Korea. His research interests include computational fluid dynamics and aerial application technology.